Ablation and ultrafast dynamics of zinc selenide under femtosecond laser irradiation

Xiaofeng Wang (王晓峰), Tianqing Jia (贾天卿), Xiaoxi Li (李晓溪), Chengbin Li (李成斌), Donghai Feng (冯东海), Haiyi Sun (孙海轶), Shizhen Xu (徐世珍), and Zhizhan Xu (徐至展)

State Key Laboratory of High Field Laser Physics,
Shanghai Institute of Optics and Fine Mechanics, Chinese Academy of Sciences, Shanghai 201800

Received January 28, 2005

The ablation in zinc selenide (ZnSe) crystal is studied by using 150-fs, 800-nm laser system. The images of the ablation pit measured by scanning electronic microscope (SEM) show no thermal stress and melting dynamics. The threshold fluence is measured to be 0.7 J/cm^2. The ultrafast ablation dynamics is studied by using pump and probe method. The result suggests that optical breakdown and ultrafast melting take place in ZnSe irradiated under femtosecond laser pulses.

OCIS codes: 320.7130, 320.2250, 350.1820.

The study on femtosecond laser-material interaction, especially the topics of laser ablation theorem and ultrafast dynamics in the process[1−9], has been a very rich subject in the last few decades. The spotlights are confined to metal[4,5,9], transparent material[7], IV semiconductors[2], and III-V compounds[3,6,8], rather than the II-VI compounds[10]. ZnSe is an important luminescent II-VI semiconductor material, with a band gap of 2.7 eV. Its transmission range is 0.5—22 μm, and it is considered as a promising semiconductor for the fabrication of blue/green laser diodes (LDs) and photoelectronic devices[11,12].

In this letter, the ZnSe ablation results under irradiation of 800-nm femtosecond lasers with varied pulse energy and width are presented. According to the logarithmical relationship between the ablation area and laser energy, the femtosecond laser ablation threshold is measured. We also discuss the advantages of femtosecond laser ablation in ZnSe crystal. With a pump-probe technique, the ultrafast dynamic processes, including electron excitation, phase-transmission and cooling, are also explored.

The experimental setup used in this work is illustrated in Fig. 1. The pump and probe beams are generated by a Ti:sapphire laser at a wavelength of 800 nm. The beam first goes through a half-wave plate and a polarizer so that the laser energy is controllable in the range of 0—0.7 mJ. The probe beam passes through a delay line and is then aligned collinear with pump beam. Both laser beams are focused with a lens onto the ZnSe sample which is mounted on an x-y-z translation stage at a near-normal angle. The sample is undoped single-crystal ⟨100⟩ wafer with a thickness of 2 mm, and it is polished on both sides with roughness less than 15 nm. The probe beam reflected at surface is spectrally separated from the scattered pump beam by a prism, and detected by a photomultiplier. The change on the surface is video monitored using a charge-coupled device (CCD) camera.

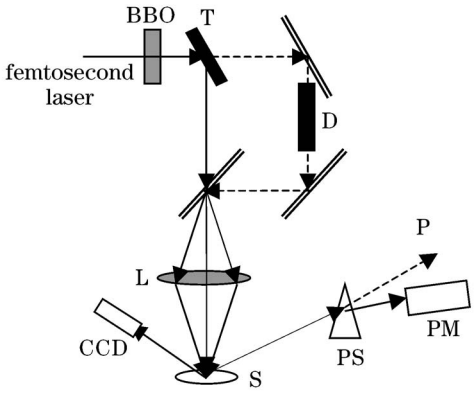

Fig. 1. Schematic of the pump-probe setup. T: 800 nm transmission and 400 nm reflection; L: lens; PS: prism; PM: photomultiplier; P: pump light; S: sample; D: delay line.

The high-quality beam and the absence of heat diffusion and melting result in a regular morphology of the damaged spots (see Fig. 2). The white ring results from the change of material lattice structure. The most serious damage always occurs at the location corresponding to the peak of the Gaussian spatial profile. For long pulses, the damage is thermal in nature and characterized by the melting and boiling of the surface. But for femtosecond laser pulses, there is no evidence of typical thermal damage such as cracks, ripples, columns, and recast layers, which are frequently observed in picosecond or nanosecond laser ablation. The short duration also means that the hydrodynamic motion of the matter

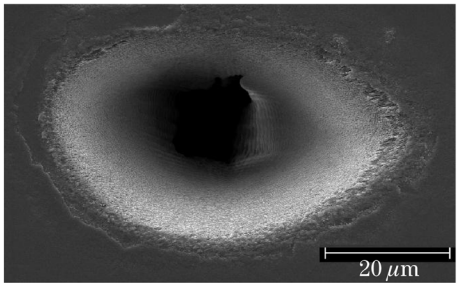

Fig. 2. Scanning electron micrograph (SEM) of front-surface damage on ZnSe crystal produced by 150-fs pulse with 500 shots with a pulse energy of 20 μJ.

under laser irradiation can be ignored, and there is essentially no fluid dynamics to be considered during the femtosecond laser-material interaction. Under femtosecond laser irradiation, ultrafast energy deposition with laser pulses vaporizes and ablates the illuminated volume before thermal relaxation happens. Because most of the deposited energy is removed in the ablated material, the surrounding remains unaffected, leaving clear boundaries, improving the spatial resolution of processed structures[13]. Femtosecond laser ablation realizes the real "cool" micromachining, assuring a smoother and regular machining surface, and a finer micromachining process. Femtosecond laser micromachining is assumed to impulse the development of the nanometer scale manufacturing technology.

With the method first developed by Liu *et al.*[14], the logarithmical relationship between the ablation area and laser energy determines that the fluence is the so-called ablation threshold when the ablation area is extrapolated to zero. With the above idea, the ablation threshold of ZnSe crystal under irradiation of 150-fs laser is measured as 0.7 J/cm^2 (see Fig. 3).

A phenomenological two-step model of the phase transition is proposed to understand the ultrafast dynamics of ZnSe under femtosecond laser irradiation[15]. There is an initial excitation stage in which under the irradiation of femtosecond laser the change of the optical reflectivity is caused by electronic excitation, while the material lattice undergoes no structural change. The excitation stage is limited by the duration of the laser pulse. And it is followed by a transition stage in which the material softens to the liquid phase. The transition stage may last for several hundred femtoseconds or even longer, depending on the laser excitation.

When the crystal is irradiated by laser above the ablation threshold, the electron-hole plasma density reaches 10^{22} cm^{-3} or higher, depending on the pump beam intensity. Owing to ultrafast carrier-carrier scattering, the initial electronic energy distribution relaxes to a thermal distribution soon, and the carrier temperature reaches a scale of 10^4 K. The relation between dielectric function of material $\varepsilon^*(\hbar\omega)$ and the optical reflectivity can be described as[16]

$$\varepsilon^*(\hbar\omega) = 1 + [\varepsilon_g(\hbar\omega + \Delta E_{gap}) - 1]\frac{N_0 - N_{e-h}}{N_0} - \frac{N_{e-h}e^2}{\varepsilon_0 m^*_{opt} m_e \omega^2}\frac{1}{1 + i\frac{1}{\omega\tau_D}}, \quad (1)$$

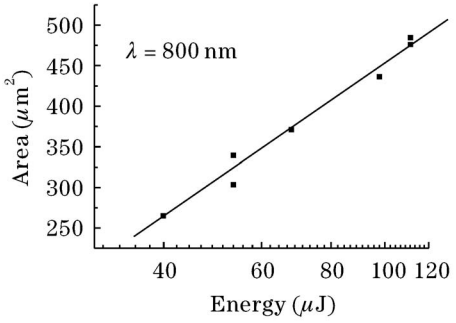

Fig. 3. Determination of the threshold fluence from the dependence of damaged area on laser pulse energy.

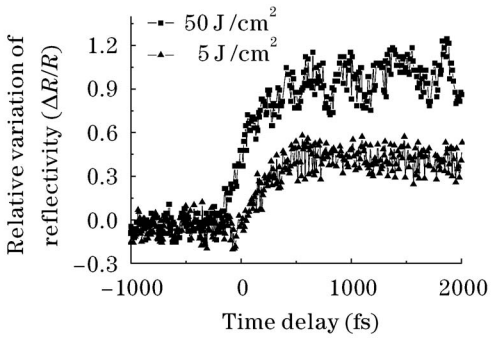

Fig. 4. Reflectivity in the excitation stage as a function of delay time for different laser fluences above the melting threshold.

where ε_g is the dielectric constant of the unexcited material, ΔE_{gap} is shrinkage of the energy gap, m_e is the mass of electrons, N_0 and N_{e-h} are the densities of the total valent band electron and electron-hole plasma, m^*_{opt} denotes the optical effective mass of the carriers, and τ_D is the Drude damping time.

In the excitation stage the optical reflectivity shown in Fig. 4 rises sharply. The zero time delay corresponds to the overlap of pump and probe pulses. A minus time delay indicates that the probe pulse reaches the sample before the pump pulse. The energy of a photon of 400-nm laser is larger than the band gap of ZnSe, and a valent band electron can jump to the conduction band with single photon absorption, creating a hole at the same time. The maximum reflectivity relates to the pulse energy. At the zero point there is no obvious rise for the reflectivity with 5-J/cm^2 pump pulse, but a 50% increase for the 50-J/cm^2 pump pulse. When the pump energy increases, there is a linear rise for the conduction band electron density for single photon absorption, resulting in the rapid ascent of reflectivity.

The excitation stage is followed by a transition of the excited solid to a quasi-liquid state. The continuous rise of reflectivity can be interpreted with the superheated melting and the maximum reflectivity corresponds to the formation of a thin liquid layer on the surface[17]. With the diffusion of energy, the temperature decreases. The cooling and resolidification of material result in the change of lattice structure, accompanying the decline of reflectivity.

Figure 5 shows the reflectivity as a function of time delay with various pump fluence. With the increase of electron-hole density, the reflectivity undergoes a slight decrease and then a rapid increase. After a slow decay of tens of picoseconds, the reflectivity comes down to a position lower than the original value. The pump fluence influences the change of reflectivity, 50% rise for 5-J/cm^2 pump beam, but 120% rise for 50-J/cm^2 pump beam. When the pump energy is far above the threshold, the ablation process is shortened, and the thermal effect is reduced (see Fig. 2). Under the irradiation of long pulses, the process of ablation lasts for tens of nanoseconds, and the ablation area expands with the diffusion of energy[18]. While for femtosecond laser ablation, the process of material heating, splashing, melting, and cooling lasts for only 20 ps, and the whole process does not prolong with the increase of pump energy. So the diffusion of energy

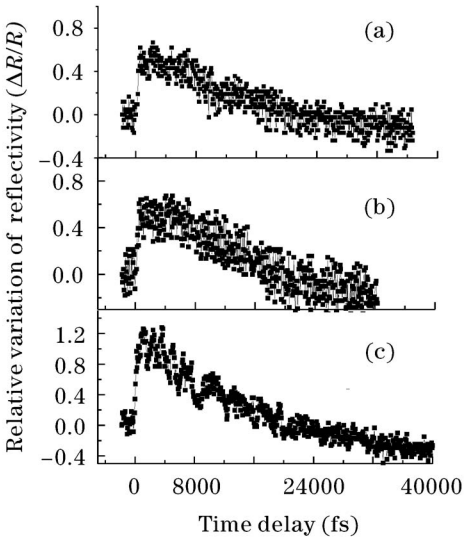

Fig. 5. Reflectivity as a function of delay time for various laser fluences of 5 (a), 10 (b), and 50 J/cm^2 (c).

is greatly reduced, and the micromachining precision is improved.

In summary, the 150-fs, 800-nm laser ablation in ZnSe crystal and micromachining are studied. According to the logarithmical relationship between the ablation area and laser fluence, the femtosecond laser ablation threshold is measured to be 0.7 J/cm^2. The results indicate that the damage caused by ultrashort pulse is non-thermal, different from that with long pulse. The ultrafast dynamics processes, including electron-hole plasma excitation, are also investigated by using the pump-probe technique. A strong change of the surface reflectivity expresses the optical breakdown and ultrafast melting of the crystal.

This work was supported by the National Natural Science Foundation of China under Grant No. 60108002.

X. Wang's e-mail address is dawnpeaking@siom.ac.cn.

References

1. N. Bloembergen, IEEE J. Quantum Electron. **10,** 375 (1974).
2. C. V. Shank, R. Yen, and C. Hirlimann, Phys. Rev. Lett. **50,** 454 (1983).
3. W.-Z. Lin, R. W. Schoenlein, J. G. Fujimoto, and E. P. Ippen, IEEE J. Quantum Electron. **24,** 267 (1988).
4. B. N. Chichkov, C. Momma, S. Nolte, F. von Alvensleben, and A. Tünnermann, Appl. Phys. A **63,** 109 (1996).
5. X. Zhu, D. M. Villeneuve, A. Yu. Naumov, S. Nikumb, and P. B. Corkum, Appl. Surf. Sci. **152,** 138 (1999).
6. W.-M. Liu, R.-Y. Zhu, S.-X. Qian, S. Yuan, and G.-Y. Zhang, Chin. Phys. Lett. **19,** 1711 (2002).
7. T. Q. Jia, Z. Z. Xu, R. X. Li, D. H. Feng, X. X. Li, C. F. Cheng, H. Y. Sun, N. S. Xu, and H. Z. Wang, J. Appl. Phys. **95,** 5166 (2004).
8. S. S. Prabhu and A. S. Vengurlekar, J. Appl. Phys. **95,** 7803 (2004).
9. H. Sun, Z. Xu, T. Jia, X. Li, C. Li, D. Feng, S. Xu, and X. Ge, Chin. Opt. Lett. **3,** 60 (2005).
10. N. Xu, F. Li, B.-H. Boo, J.-K. Lee, and H.-J. Cho, Chin. J. Lasers (in Chinese) **28,** 661 (2001).
11. S. Adachi and T. Taguchi, Phys. Rev. B **43,** 9569 (1991).
12. H. Gong, K. Liu, M. Wang, and H. Huang, China Ceramics (in Chinese) **39,** (3) 15 (2003).
13. M. Lenzner, J. Krüger, W. Kautek, and F. Krausz, Appl. Phys. A **68,** 369 (1999).
14. J. M. Liu, Opt. Lett. **7,** 196 (1982).
15. K. Sokolowski-Tinten, J. Bialkowski, and D. von der Linde, Phys. Rev. B **51,** 14186 (1995).
16. K. Sokolowski-Tinten and D. von der Linde, Phys. Rev. B **61,** 2643 (2000).
17. J. Bonse, S. M. Wiggins, and J. Solis, J. Appl. Phys. **96,** 2628 (2004).
18. J. Solis and C. N. Afonso, J. Appl. Phys. **69,** 2105 (1991).